Supplemental Information for:

Pyramidal neurons in prefrontal cortex receive subtype-specific forms of excitation and inhibition

Anthony T. Lee* [1,2,3], Steven M. Gee* [1,2,3], Daniel Vogt [1],

John L. Rubenstein [1], and Vikaas S. Sohal† [1,2,3]

[1]Department of Psychiatry, [2]Center for Integrative Neuroscience,

and [3]Sloan-Swartz Center for Theoretical Neurobiology

University of California, San Francisco

675 Nelson Rising Lane

San Francisco, CA 94143-0444

* These two authors contributed equally to this work

SUPPLEMENTAL FIGURE CAPTIONS

FIGURE S1. Classification of Type A and B neurons, and differences between callosal EPSPs in Type A and B neurons, Related to Fig. 1. (A) Classification of Type A and Type B neurons based on a combination of the sag and rebound in response to a -250 pA pulse, and the afterhyperolarization (AHP) following a +250pA current pulse. Type A neurons were classified as cells with combined values >6.5 mV (dotted line). **(B)** Application of TTX and 4-AP eliminates excitatory responses to optogenetic stimulation of callosal projections. **(C)** EPSP dynamics in simultaneously recorded Type A and B neurons in cases that failed to evoke circuit inhibition (n = 3 pairs). These experiments have a similar latency to EPSP peak as our other experiments (15.4 ± 2.1 msec in these experiments, compared to 13.8 ± 1.8 msec in our complete dataset; p = 0.64). In these experiments, the difference between the pattern of EPSPs in Type A and B neurons was also similar to our other experiments. Specifically, the ratio between the second and first response was 1.57 ± 0.57 in Type A cells, and 0.77 ± 0.13 and in Type B cells, compared to 1.25 ± 0.18 and 0.78 ± 0.15 respectively in our complete dataset**. (D)** Representative image of Type A (green) and Type B (red) neurons labeled with retrogradely transported fluorescent microspheres injected into the MD thalamus (red) and contralateral mPFC (green), respectively. **(E)** Current clamp responses of labeled Type A (coticothalamic, CT) and B (cortiocallosal, CC) neurons to injection of -250pA. **(F)** Optogenetic stimulation of callosal inputs elicit depressing EPSPs in labeled Type B (CC) neurons, but not in labeled Type A (CT) neurons.

FIGURE S2. Blocking post-synaptic voltage-dependent Ca^{2+} channels and NMDARs does not alter EPSP dynamics in Type A neurons, Related to Fig. 2. (A) Application of mibefradil (5 μM) + nimodipine (5 μM) + AP5 (50 μM) does not alter EPSP dynamics in Type A during optogenetic stimulation of callosal inputs (n = 4). **(B)** The paired-pulse ratio is not significantly different after applying these Ca^{2+} channel blockers (p = 0.19, n = 4).

FIGURE S3. **Blocking h-current has minimal effects on simulated EPSPs and spiking in Type A neurons, Related to Fig. 3. (A)** ZD7288 (25 μM) blocks I_h in Type A neurons. **(B)** ZD7288 (brown) has minimal effects on the current clamp responses of Type A neurons to injection of Type A or B current waveforms (averaged response shown in black, individual responses shown in gray). **(C)** The paired-pulse ratio during responses of Type A neurons to simulated EPSCs in these current waveforms is not significantly altered by blocking I_h current (p = 0.30 and 0.39 for Type A and B waveforms, respectively; n=4 cells). **(D)** Blocking I_h with ZD7288 also fails to significantly alter the amount of spiking in Type A neurons in response to scaled up, suprathreshold current waveforms (p = 0.79 and 0.13 for Type A and B waveforms, respectively; n=4 cells).

FIGURE S4. Effects of blocking $GABA_A$Rs on EPSPs, and measuring inhibitory inputs to Type A and B neurons, Related to Fig. 4. (A) *A1:* Picrotoxin (ptx; 10 μM) blocks outward currents that follow optogenetic stimulation of callosal inputs and represent feedforward inhibition in Type A neurons. *A2:* Ptx application prolongs EPSPs in Type A neurons evoked by optogenetic stimulation of callosal inputs. Thick lines represent the averaged EPSPs before (black) and after (red) ptx application. Before averaging, each EPSP trace was normalized by

the average amplitude of control EPSPs in that cell. Thin lines show individual normalized responses. *A3:* Ptx significantly prolongs the decay time constant for callosal EPSPs in Type A neurons (n=4 cells; $p<0.001$ by repeated measures ANOVA). **(B)** The dynamics of callosal EPSPs in Type A neurons are not significantly altered by application of ptx (black). To avoid epileptiform discharges, the light power was reduced to ~0.2 mW/mm^2, i.e. 10% of the typical power, for some of these experiments. Spikes during responses in ptx have been truncated. **(C)** Ptx does not significantly alter the paired-pulse ratio for Type A neuron responses to optogenetic stimulation of callosal inputs ($p = 0.37$, n=4 cells). **(D)** Inhibitory currents peak ~2 msec after excitatory currents during optogenetic stimulation of callosal inputs ($p < 0.01$). **(E)** The average distance between FSINs and Type A or B neurons during experiments to measure connectivity from FSIN to these two subtypes ($p = 0.271$). **(F)** Experimental design: We simultaneously recorded from a pair of Type A (red) and B (blue) neurons in SOM::Cre mice injected with virus to drive Cre-dependent ChR2-EYFP expression (orange). During optogenetic stimulation of ChR2-expressing SOM interneurons, we recorded simultaneous IPSCs in Type A and B neurons in voltage clamp at +10 mV (bottom). **(G)** The peak amplitude of SOM interneuron-mediated IPSCs (left) and the corresponding inhibitory charge transfer (right) were similar in Type A and B neurons ($p = 0.6$ and $p = 0.8$, respectively; n=7 pairs).

FIGURE S1

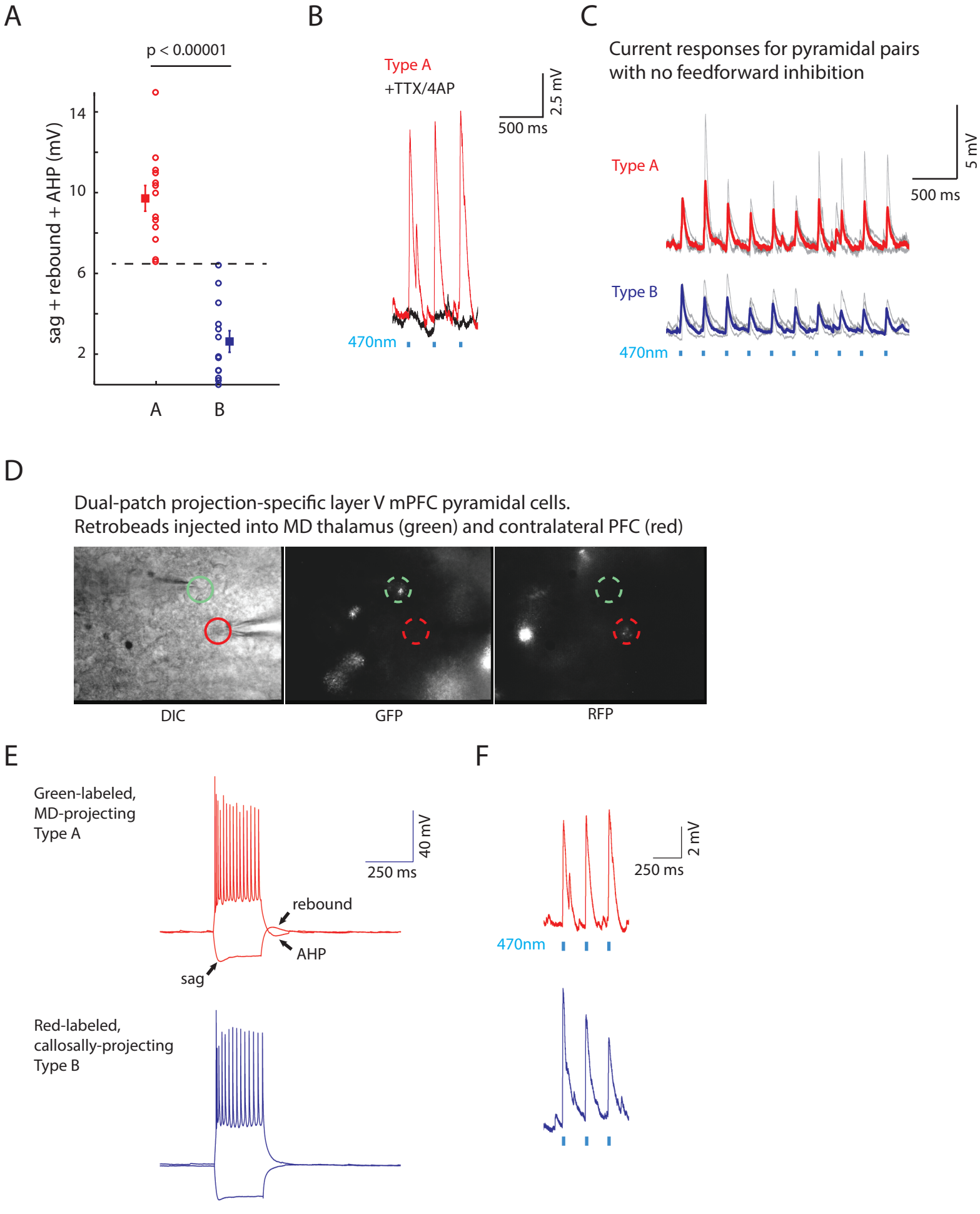
A
p < 0.00001
sag + rebound + AHP (mV)
14
10
6
2
A
B
B
Type A
+TTX/4AP
2.5 mV
500 ms
470nm
C
Current responses for pyramidal pairs
with no feedforward inhibition
Type A
5 mV
500 ms
Type B
470nm
D
Dual-patch projection-specific layer V mPFC pyramidal cells.
Retrobeads injected into MD thalamus (green) and contralateral PFC (red)
DIC
GFP
RFP
E
Green-labeled,
MD-projecting
Type A
40 mV
250 ms
rebound
AHP
sag
Red-labeled,
callosally-projecting
Type B
F
2 mV
250 ms
470nm

FIGURE S2

A

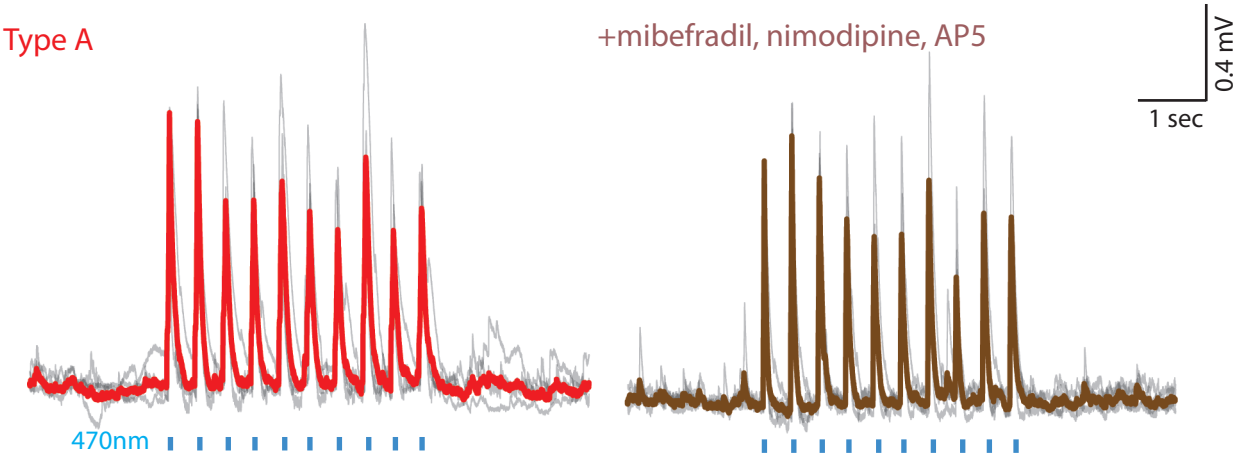
Type A
+mibefradil, nimodipine, AP5
0.4 mV
1 sec
470nm

B

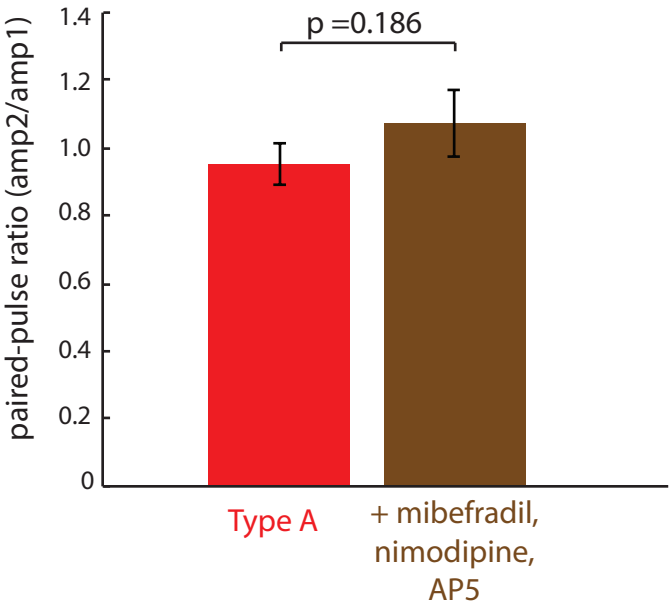
p =0.186
paired-pulse ratio (amp2/amp1)
1.4
1.2
1.0
0.8
0.6
0.4
0.2
0
Type A
+ mibefradil, nimodipine, AP5

FIGURE S3

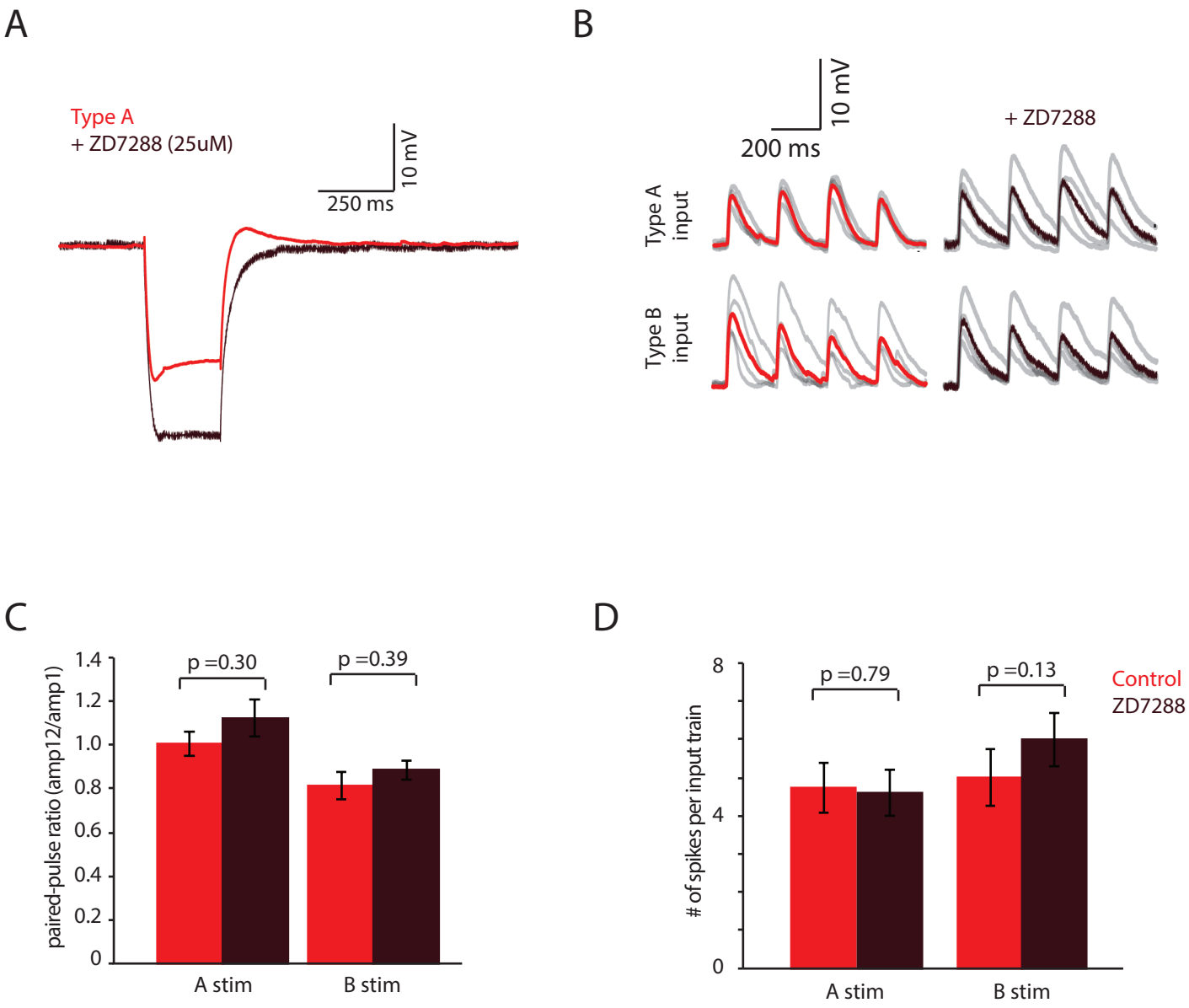
A
Type A
+ ZD7288 (25uM)
10 mV
250 ms
B
10 mV
200 ms
+ ZD7288
Type A input
Type B input
C
paired-pulse ratio (amp12/amp1)
1.4
1.2
1.0
0.8
0.6
0.4
0.2
0
p =0.30
p =0.39
A stim
B stim
D
# of spikes per input train
8
4
0
p =0.79
p =0.13
Control
ZD7288
A stim
B stim

FIGURE S4

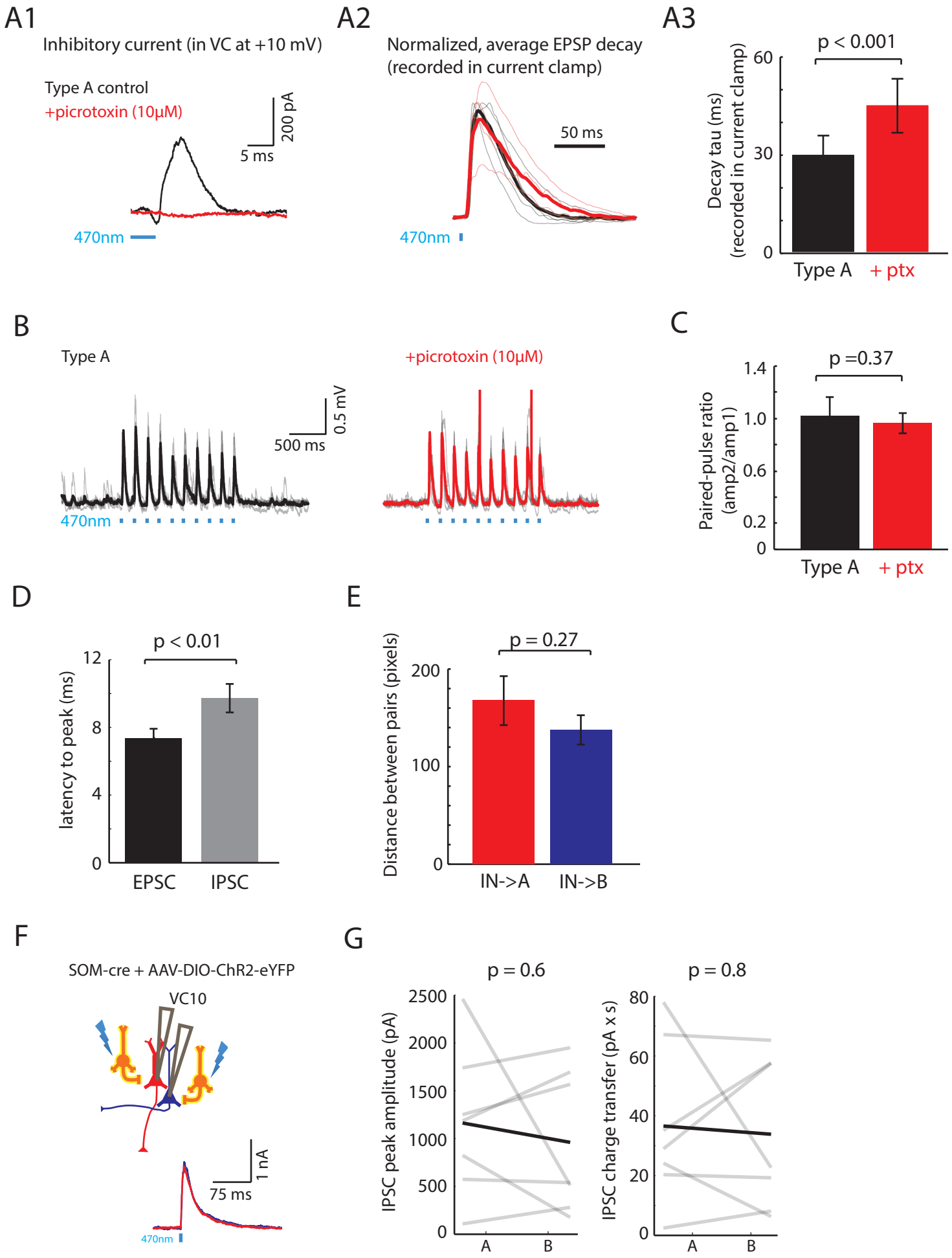
A1
Inhibitory current (in VC at +10 mV)
Type A control
+picrotoxin (10μM)
200 pA
5 ms
470nm
A2
Normalized, average EPSP decay
(recorded in current clamp)
50 ms
470nm
A3
p < 0.001
Decay tau (ms)
(recorded in current clamp)
60
30
0
Type A
+ ptx
B
Type A
+picrotoxin (10μM)
0.5 mV
500 ms
470nm
C
p =0.37
Paired-pulse ratio
(amp2/amp1)
1.4
1.0
0.6
0.2
0
Type A
+ ptx
D
p < 0.01
latency to peak (ms)
12
8
4
0
EPSC
IPSC
E
p = 0.27
Distance between pairs (pixels)
200
100
0
IN->A
IN->B
F
SOM-cre + AAV-DIO-ChR2-eYFP
VC10
1 nA
75 ms
470nm
G
p = 0.6
p = 0.8
IPSC peak amplitude (pA)
2500
2000
1500
1000
500
0
A
B
IPSC charge transfer (pA x s)
80
60
40
20
0
A
B